Journal of Organometallic Chemistry 694 (2009) 3343–3348

Contents lists available at ScienceDirect

Journal of Organometallic Chemistry

journal homepage: www.elsevier.com/locate/jorganchem

Mechanistic investigation on hydrogenation and hydrosilylation of ethylene catalyzed by rhenium nitrosyl complex

Lingjun Liu, Siwei Bi *, Min Sun, Xiangai Yuan, Ning Zheng, Ping Li

College of Chemistry and Chemical Engineering, Qufu Normal University, 57 Jingxuan West Road, Qufu, Shandong 273165, China

ARTICLE INFO

Article history:
Received 24 February 2009
Received in revised form 22 May 2009
Accepted 26 May 2009
Available online 6 June 2009

Keywords:
Hydrogenation
Hydrosilylation
Rhenium nitrosyl complex
Ethylene

ABSTRACT

The mechanistic study for hydrogenation and hydrosilylation of ethylene catalyzed by a rhenium nitrosyl complex is carried out with the aid of density functional theory computations. The hydrogenation of ethylene is found to be available kinetically in which the oxidative addition of H_2 plays a role in decreasing the reaction barrier. For the case of hydrosilylation of ethylene, it is found the oxidative addition of $HSiMe_3$ cannot occur due to steric reasons, instead, a σ-bond metathesis process for reductive elimination of $C_2H_5SiMe_3$ is proposed. The major reason for the inaccessibility for the hydrosilylation is resulted from the fact that the oxidative addition of $HSiMe_3$ cannot give a more stable intermediate.

1. Introduction

Homogeneous hydrogenation of organic substrates such as olefin, alkyne, etc. is the most widely studied class of catalyzed organometallic reactions [1–9]. The key step of these processes is the activation of H_2 by organotransition complexes. Experimental and theoretical studies on the interaction of H_2 molecule with a metal center have provided valuable insight into how the activation of the H–H bond might occur [10]. The metal hydride complexes formed from the activation of H–H normally undergo insertion or hydride transfer reactions with a wide variety of unsaturated compounds to finish hydrogenation. However, the M–H bond in many cases appears to be quite strong and reluctant to undergo the aforementioned types of reaction. Therefore, it was concerned how ancillary ligands are able to influence the M–H bond and subsequently activate it.

NO is known to be a non-innocent ligand able to support different oxidation states of metal centers and showing different coordination modes. Furthermore, it exerts a relatively strong trans-influence or trans-effect, thus leading to metal–ligand bonds activated [11–14]. Special attention was paid to nitrosyl complexes [15–20]. Berke and his group have studied the chemistry of nitrosyl-substituted transition metal hydrides [21–23] in recent years such as *trans*-$W(CO)_2H(NO)(PR_3)_2$, $Re(CO)H_2(NO)(PR_3)_2$, $MnH(NO)_2(PR_3)_2$, $ReH(NO)_2(PR_3)_2$, and demonstrated that the nitrosyl ligand can activate the M–H bond and induce a quite strong hydridic polarization. The CO ligand is normally regarded as a weaker π-acceptor ligand than NO ligand, and the carbyne ligand CR(R = alkyl, aryl) is regarded as a three electron donor and a good π-accept like the linear NO ligand, so how this ancillary ligands might influence the M–H bond also have been studied [11,13,24–28].

Berke and his group recently reported several examples of rhenium mono- and dinitrosyl complexes that are active in hydrogenation and hydrosilylation of unsaturated organic molecules [29,30]. They also studied the ethylene chemistry of Re(I) mononitrosyl hydride complexes [31], which demonstrated the general disposition to coordinate ethylene and to undergo organometallic reactions. Although the chemistry and the catalytic potential of such complexes have been explored, few detailed theoretical studies are focused on the reaction mechanisms for hydrogenation and hydrosilylation of alkenes catalyzed by Re(I) mononitrosyl hydride complexes. As mentioned above, the role of nitrosyl has been explored in details. In this paper, our interest is not to investigate the influence of nitrosyl on the activation of H–H, instead, but is to make effort to explore the reaction mechanisms for hydrogenation and hydrosilylation of alkenes catalyzed by Re(I) mononitrosyl hydride complexes with the aid of density functional theory (DFT) calculations. The title reactions are chosen as shown in Eq. (1). We hope this work would present some detailed understanding for hydrogenation and hydrosilylation catalyzed by rhenium nitrosyl transition metal complexes and provide further information for experimentalists.

$$H{-}R' + H_2C{=}CH_2 \xrightarrow[\left(R={}^{i}Pr,cy;R'=H,Si(Me)_3\right)]{Re(H)_2(\eta^2\text{-}C_2H_4)(NO)(PR_3)_2} H_3C{-}CH_2R' \qquad (1)$$

* Corresponding author. Fax: +86 537 4456305.
E-mail address: siweibi@126.com (S. Bi).

0022-328X/$ - see front matter © 2009 Elsevier B.V. All rights reserved.
doi:10.1016/j.jorganchem.2009.05.038

2. Computational details

In our calculations, we optimized all molecular geometries at the Becke3LYP(B3LYP) level of density functional theory (DFT) [32–34]. In order to identify all stationary points as minima (zero imaginary frequencies) or transition states (one imaginary frequency) and to provide free energies at 298.15 K which include entropic contributions by taking in account the vibrational, rotational and translational motions of the species under consideration, we calculated frequencies at the same level of theory. All the transition states were checked by IRC (Intrinsic Reaction Coordinate) analysis [35,36]. To describe Re, Si and P atoms we use the effective core potentials (ECPS) of Hay and Wadt with double-ζ valence basis sets (LanL2DZ) [37], and to describe C, N, O, H atoms we use standard 6-31G basis sets. Polarizations functions were added for H (H1, H2, H3, H4 $\zeta(p) = 0.11$) and those atoms directly involved in bond-forming and bond-breaking processes, C (C1, C2 $\zeta(d) = 0.8$), Si($\zeta(d) = 0.262$) and P($\zeta(d) = 0.34$) [38]. All the transition metal complexes involved in this work are found in singlet state. All the calculations were performed with the GAUSSIAN 98 software package [39]. The computational method and the basis sets used in this work have been widely used and recognized in theoretically studying the bonding, structures and reaction mechanisms of organometallic systems [40–46]. To test the validity of the basis sets used in this work, we carry out single-point calculations of the species in a selected reaction step using better basis sets of SDD with all-polarized basis set. The results show that the difference between two basis sets is small. For example, with LanL2DZ, the free energies and relative electronic energies (in parenthesis) of **R**, **TS1**, **Int1**, **TS2** and **Int2** are 0.0 (0.0), 20.8 (23.1), 10.4 (10.6), 12.1 (12.6) and 11.6 (8.9), and with SDD, the corresponding data are 0.0 (0.0), 22.5 (23.9), 11.5 (11.1), 13.3 (13.5) and 12.6 (13.0). In this work, we choose alkene as a substrate to undergo hydrogenation and hydrosilylation. $Re(H)_2(\eta^2\text{-}C_2H_4)(NO)(PR_3)_2$ (R = ^{i}Pr, Cy) is employed as a catalyst. For saving computational time, the catalyst is modeled by replacing the ^{i}Pr group with methyl to give the model catalyst, $Re(H)_2(\eta^2\text{-}C_2H_4)(NO)(PMe_3)_2$ (**Cat**). The previous similar theoretical study indicates the modeling of the catalyst is reasonable [47–49].

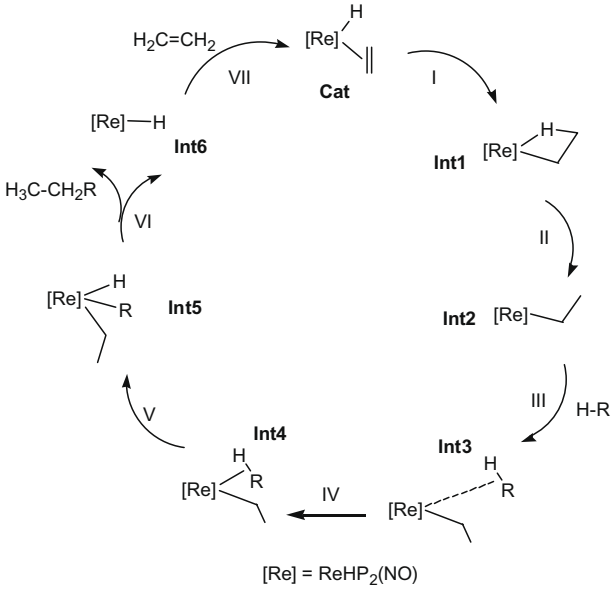

Scheme 1. Theoretically proposed catalytic cycle for hydrogenation and hydrosilylation of ethylene catalyzed by the rhenium nitrosyl complex (**Cat**) (P = PMe_3, R = H, $SiMe_3$).

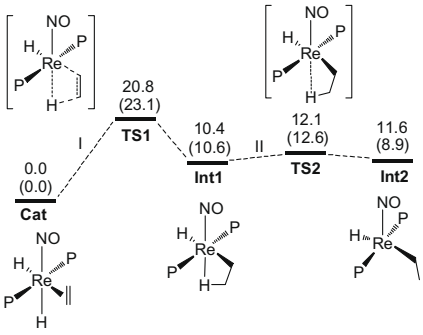

Fig. 1. Free energy profile for insertion of ethylene into Re–H bond. The free energies and electronic energies (in parentheses) are given in kcal/mol (P = PMe_3).

3. Results and discussion

On the basis of the experimental observations, the catalytic cycle is theoretically proposed as shown in Scheme 1. The first step is the ethylene insertion into the Re–H bond followed by the breaking of the agostic interaction involved in **Int1** to afford **Int2** (step II). Steps III and IV are associated with the coordination of the substrate H–R to give a σ complex (**Int4**). Step V involves an oxidative addition process of H–R to the metal center to generate a seven-coordinate complex (**Int5**). Step VI leads to the formation of the product $H_3C\text{–}CH_2R$ by a reductive elimination process. The catalyst **Cat** is regenerated by coordination of ethylene to **Int6** in the final step (step VII), completing the whole catalytic cycle. The following sections are the detailed investigations on the mechanisms of hydrogenations and hydrosilylation of ethylene catalyzed by the rhenium nitrosyl complex (**Cat**).

3.1. Mechanistic study on hydrogenation of ethylene

3.1.1. Insertion of ethylene into Re–H bond

The free energy profile for insertion of ethylene into Re–H bond is shown in Fig. 1. The structural parameters for selected species involved in the free energy profile are shown in Fig. 4. Relative free energies are used to analyze the reactive mechanism. But this Gibbs free energy was evaluated in gas phase. The entropic contribution to the free energies based on the gas phase calculation is overestimated in solution. Recent discussions on the overestimation can be found on literature [50,51]. It is found the ethylene ligand is parallel to the P–Re–P axis while not parallel to the ON–Re–H axis in the optimized geometry of the catalyst **Cat**. That means, as the ethylene inserts into the Re–H bond, the ethylene has to rotate around the Re–centroid of ethylene to afford a nearly square planar structure with the adjacent Re–H bond. The barrier is found to be quite high (>20 kcal/mol). Maybe the rotation of the ethylene is a factor in increasing the activation energy. A Re···H–C agostic interaction is involved in **Int1**, which is supported by the structural parameters (Re–H1: 2.08 Å, Re–C2–C1: 85°, C1–H1: 1.16 Å). In step II, the cleavage of the Re···H–C agostic bond is found quite facile, as demonstrated by the very small activation energy (1.7 kcal/mol in free energy), indicating the agostic interaction is very weak. **Int2** is less stable than **Cat** since the former is a 16e species while the latter is an 18e species. On the whole, the insertion of ethylene into the Re–H bond is unfavorable thermodynamically.

3.1.2. Oxidative addition of H_2 to Re center

In this part, we first discuss the oxidative addition of H_2. The oxidative addition of H–$SiMe_3$ will be discuss in the later section. Based on the geometric structure of **Int2**, two possible directions

of H_2 attack at the metal center can be proposed. One is from between the hydride and the ethyl (path I), and the other is from between the nitrosyl and the ethyl (path II). The calculated energy profiles are shown in Fig. 2. The structural parameters for selected species involved in the two free energy profiles are shown in Fig. 4.

Int3 and **Int3′** are formed by the fan de Waals interaction between **Int2** and H_2. The higher free energies of **Int3** and **Int3′** compared to **Int2** are due to the entropy increase. **Int3** is less stable than **Int3′** due to the strong trans-influence of the hydride to the ethyl in trans position. The steps IV and IV′ are the coordination of H_2 to give **Int4** and **Int4'** respectively. Calculated results show that the energy difference between **Int4** and **Int4'** is 11.8 kcal/mol, indicating the former is markedly less stable than the latter. The main reason for their different stabilities is a result of the high trans-influence of the ligand NO. Due to the trans-influence of NO to H3–H4 in **Int4**, the interaction between Re and H3–H4 is weaker than that in **Int4′** where H3–H4 is cis to NO. As seen from the geometric structures of the two intermediates, the bond distance of Re–H3 and Re–H4 in **Int4** is 1.98 Å while that in **Int4′** is 1.83 Å. Correspondingly, the bond distance of H3–H4 (0.79 Å) in **Int4** is shorter than that (0.90 Å) in **Int4′**. In other words, the dihydrogen is less activated in **Int4** than in **Int4′**. For the following H_2 oxidative addition to generate two hydrides, the barrier in energy (5.1 kcal/mol) in path I is calculated to be higher than that (0.6 kcal/mol) in path II, since the H_2 is less activated in **Int4** than **Int4′**. Examining the geometries of **Int5** and **Int5′**, one can see both of them have a pseudo pentagonal bipyramidal structure. In **Int5**, the nitrosyl and H3 occupy the two axial trans positions, and **Int5′** the nitrosyl and the ethyl occupy the two axial trans positions. Since the trans-influence of the hydride H3 to NO in **Int5** is stronger than that of the ethyl to NO in **Int5′**, the former becomes less stable than the latter. In summary, the H_2 oxidative addition can undergo two different pathways based on the different attacking directions of H_2 at the metal center.

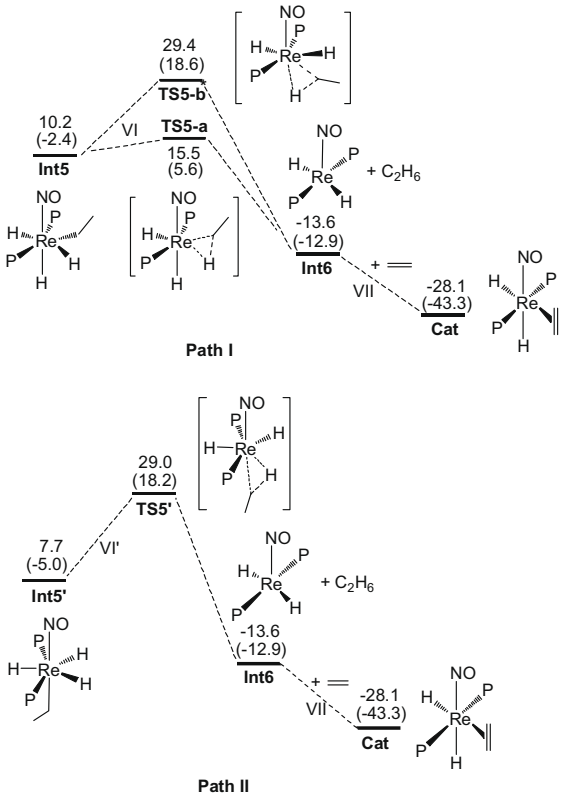

Fig. 3. Free energy profile for reductive elimination of C_2H_6 and the regeneration of the catalyst. The free energies and electronic energies (in parentheses) are given in kcal/mol (P = PMe_3).

3.1.3. Reductive elimination of C_2H_6 and regeneration of the catalyst (*Cat*)

The free energy profiles for reductive elimination of C_2H_6 and regeneration of the catalyst are shown in Fig. 3, and the structural parameters for selected species involved in the free energy profile are illustrated in Fig. 4. Following **Int5**, the reductive elimination of C_2H_6 was proposed theoretically going through two possible paths (see path I in Fig. 3). One is the coupling of H3 with the ethyl (via **TS5-b**) and the other is the coupling of H4 with the ethyl (via **TS5-a**). In **TS5-b**, H3 occupies one apical position. The ethyl has to significantly move away from the equatorial plane to couple with H3, making the transition state strongly distorted and lying in high energy. In **TS5-a**, both H4 and the ethyl are present in the equatorial plane. For coupling of H4 and the ethyl, the bond angle H4–Re–C2 is just needed to become smaller and the ethyl is still present in the equatorial plane. Therefore, the structure of **TS5-a** is just slightly distorted, making it much more stable compared to **TS5-b**. Calculated results and the discussion above suggest that the coupling of the ethyl with the equatorial hydride is preferred over with the apical hydride. IRC confirmed that both the two paths give the same intermediate (**Int6**). The free energy difference is calculated to be −23.8 kcal/mol, indicating the reductive elimination of C_2H_6 from **Int5** is favorable thermodynamically.

In **Int5′**, the ethyl occupies one apical position. The coupling between the ethyl and H3 is equivalent to that between the ethyl and H4. It is found, based on our calculated results, the coupling between the ethyl and H2 could not give **Int6**. So, only the coupling between the ethyl and H4 is investigated here. The barrier in free energy is calculated to be high (29.0 kcal/mol). This is because remarkable structural distortion arises as the apical ethyl couples with H4, leading to the transition state **TS-5′** lying in high energy. Finally, one ethylene coordinates to the metal center of **Int6** to regenerate the catalyst (**Cat**), completing the catalytic cycle. The hydrogenation of ethylene is favorable thermodynamically with −28.1 kcal/mol of the calculated free energy difference.

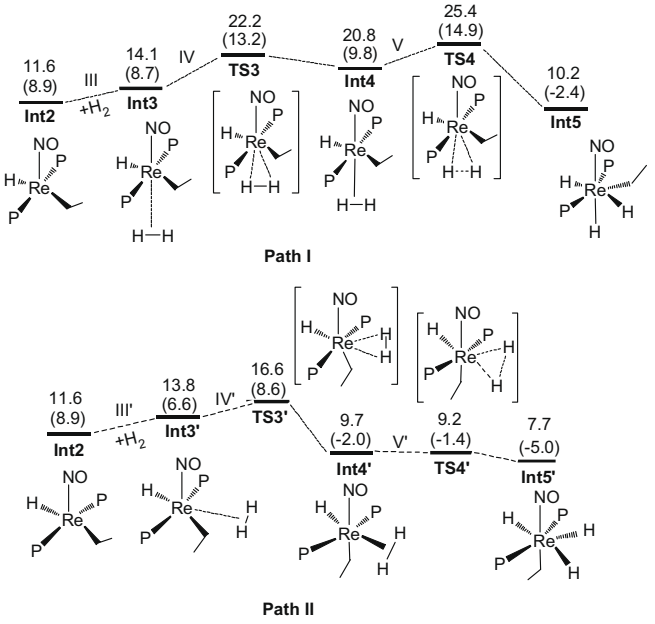

Fig. 2. Free energy profile for the oxidative addition of H_2 to Re center. The free energies and electronic energies (in parentheses) are given in kcal/mol (P = PMe_3).

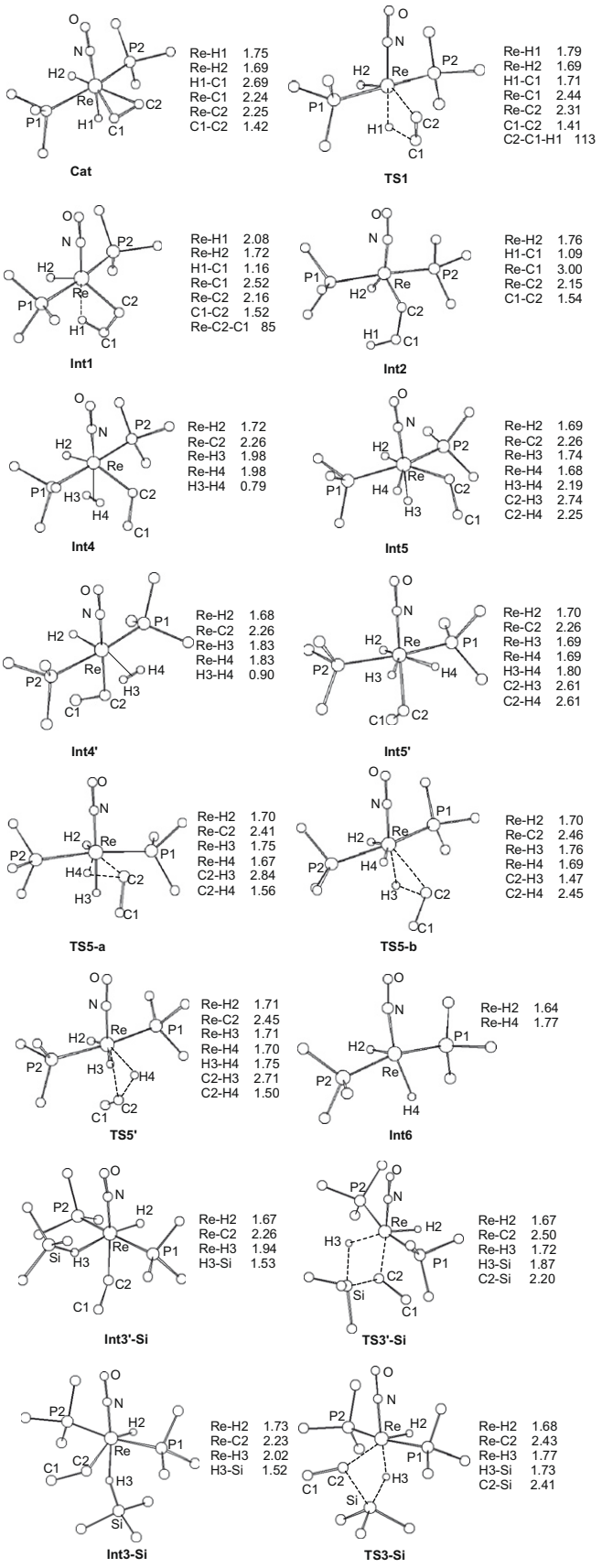

Fig. 4. B3LYP optimized structures of the selected species involved in all the free energy profiles. For clarity, the hydrogen atoms attached on ethylene and methyl groups are omitted. The bond distances are given in Å and the bond angles are given in degree.

3.2. Hydrosilylation of ethylene

As for the hydrosilylation of ethylene, the insertion of ethylene into Re–H bond is the same as shown in Fig. 1. The following steps are shown in Fig. 5, and the structural parameters are also shown in Fig. 4. The combination of **Int2** with $HSiMe_3$ gives a σ complex **Int3′–Si**. We initially proposed a pathway from **Int3′–Si** to **Int6** as illustrated in Scheme 2. The substrate $HSiMe_3$ first oxidatively adds to the metal center to afford **Int4′–Si**, then **Int6** is produced via the transition state **TS-b** in which only the ethyl and the $SiMe_3$ group couple each other. However, we cannot locate the transition state **TS-b** connecting **Int4′–Si** and **Int6**, instead the transition state **TS3′-Si** is always obtained as shown in Fig. 5. Thus, we predict that the pathway similar to the hydrogenation of ethylene as shown in Scheme 2 is not available. Instead, we proposed a pathway shown in Fig. 5 in which a σ bond metathesis process is involved. Compared with the geometric structure of **Int3′–Si**, the bonds Si–H3 and Re–C2 are elongated, and the Re–H3 and Si–C2 are shortened in the located **TS3′–Si**, indicating the former two σ bonds are being broken and the latter two σ bonds are being formed. So the step from **Int3′–Si** to **Int6** corresponds to a σ bond metathesis process. The highest barrier in free energy relative to the initial reactants is calculated to be 53.9 kcal/mol, indicating the hydrosilylation of ethylene is not available kinetically, although that is favorable thermodynamically as shown in Fig. 5. The approach of $HSiMe_3$ to Re like H2 approach leading to **Int3** and **Int5** is also examined. The transition state relevant to Si–H oxidative addition cannot be located, but the one (**TS3–Si** as shown in Fig. 5) relevant to the

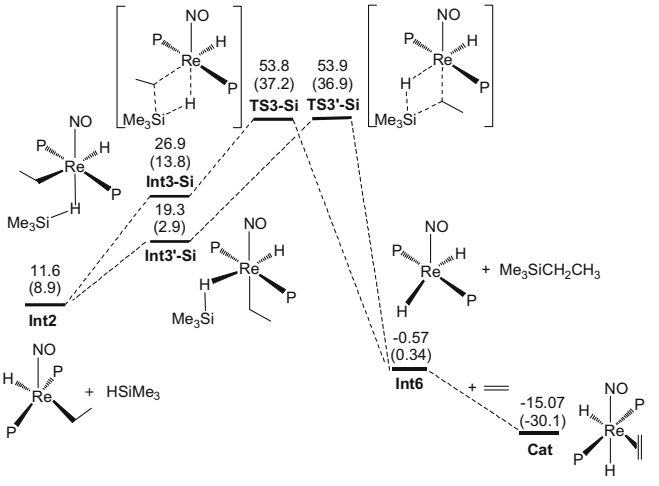

Fig. 5. Free energy profile for hydrosilylation of ethylene. The free energies and electronic energies (in parentheses) are given in kcal/mol (P = PMe_3).

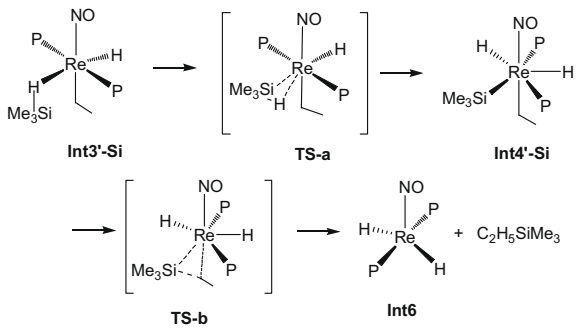

Scheme 2. (P = PMe_3).

σ-bond metathesis between Si–H and Re–C was located. The barrier for the σ-bond metathesis process is calculated to be still very high.

It is worth to compare the reaction mechanisms of the catalytic hydrogenation and hydrosilylation of ethylene. The highest free energy relative to the initial reactants is 29.0 kcal/mol for hydrogenation of ethylene while that for hydrosilylation of ethylene is 53.9 kcal/mol. This is consistent with the experimental observations that the hydrogenation can be achieved while the hydrosilylation of linear olefin is inaccessible. The reason for the availability of hydrogenation and the inaccessibility of hydrosilylation across carbon–carbon double bond of ethylene can be explained as follows. For hydrogenation of ethylene, H_2 can be oxidatively added to the catalyst to give a more stable intermediate compared with its corresponding molecular complex. As shown in Fig. 2, **Int5** and **Int5′** are respectively more stable than **Int4** and **Int4′**. For hydrosilylation of ethylene, we arbitrarily located an oxidative addition product of $HSiMe_3$ (**Int4′–Si**), and found it is less stable than the σ complex **Int3′–Si**. This is due to the fact that the $SiMe_3$ group is very bulky, making **Int4′–Si** very congested. The accessible oxidative addition of H_2 is due to the fact that hydrogen atom is very small and the valence 1s orbital is indirectional. That means the $HSiMe_3$ cannot undergo an oxidative addition to give a more stable intermediate. As our calculations shown, a transition state corresponding to σ bond metathesis (**TS3′–Si**) is always located while the arbitrarily proposed transition state **TS-b** in Scheme 2 cannot be obtained, which is also resulted from steric reasons. In view of the fact that **Int3′–Si** cannot afford an oxidative addition product, the starting point (**Int3′–Si**) undergoing reductive elimination of ethane becomes significantly higher than that (**Int5** or **Int5′**) in the case of hydrogenation of ethylene. Therefore, the highest free energy (**TS3′–Si**) relative to the initial reactants is significantly raised. Of course, the populations in the hydrogenation and hydrosilylation reactions have a large difference. As calculations show, the NBO charges on Re, C2 and H4 in **TS5-a** are −0.17320, −0.64334 and 0.10650, and that on Re, C2 and H3 in **TS3′–Si** are −1.12814, −0.82515 and −0.03700, respectively. In summary, compared the two cases of hydrogenation and hydrosilylation, the highest energy for the former case is significantly lower than the one for the latter case. The steric reasons play an important role for the kinetics of hydrogenation and hydrosilylation of ethylene.

It is to note that in all the nitrosyl Re complexes involved in this work, the unit O–N–Ir is calculated to be always linear, suggesting NO serves as a 3e donor and has the character of NO^+. Even though there exists an oxidation state change of Re in the process of hydrogenation, NO still serves as a 3e donor in order to follow 18e rule. The coordinating geometry of NO and its electronic structure do not change much.

4. Conclusions

In this paper, the mechanistic study for hydrogenation and hydrosilylation of ethylene catalyzed by a rhenium nitrosyl complex has been carried out with the aid of density functional theory computations. Catalytic hydrogenation of ethylene undergoes olefin insertion, coordination and oxidative addition of dihydrogen, reductive elimination of ethane and finally binding of ethylene to regenerate the catalyst. Two possible pathways for the hydrogenation are proposed in terms of the different attacking directions of dihydrogen. The difference of catalytic hydrosilylation from the hydrogenation of ethylene is that the $HSiMe_3$ does not undergo an oxidative addition process to afford a more stable hydrido silyl complex, instead undergoes a σ-bond metathesis process for reductive elimination of $C_2H_5SiMe_3$, leading to the barrier significantly high in free energy. The catalytic hydrogenation of ethylene is theoretically found to have relatively low reaction barriers, consistent with the experimental fact that this reaction can occur. The catalytic hydrosilylation of ethylene is theoretically found to have significantly high reaction barriers, consistent with the experimental fact that this reaction cannot occur. The reason for the phenomena is that the oxidative addition of dihydrogen can effectively give a more stable hydride complex while that of $HSiMe_3$ cannot due to steric reasons.

Acknowledgements

This work was supported by the Natural Science Foundation of Shandong Province (No. Y2007B23), the State Key Laboratory of Physical Chemistry of Solid Surfaces, Xiamen University, China (No. 200702), the Key Laboratory of Colloid Interface Chemistry, Ministry of Education, Shandong University (No. 200706) and the Scientific Research Foundation of Qufu Normal University (XJ200807).

References

[1] R. Hartmann, P. Chen, Angew. Chem., Int. Ed. 40 (2001) 3581.
[2] T.X. Le, J.S. Merola, Organometallics 12 (1993) 3798.
[3] H.M. Lee, T. Jiang, E.D. Stevens, S.P. Nolan, Organometallics 20 (2001) 1255.
[4] J.A. Osborn, F.H. Jardine, J.F. Young, G. Wilkinson, J. Chem. Soc. A (1966) 1711.
[5] A.J. Sandee, J.N.H. Reek, P.C.J. Kamer, P.W.N.M. van Leeuwen, J. Am. Chem. Soc. 123 (2001) 8468.
[6] K.T. Wan, M.E. Davis, Tetrahedron: Asymmetr. 4 (1993) 2461.
[7] G.J. Kubas, Metal Dihydrogen and ó-Bond Complexes, Kluwer Academic/Plenum, New York, 2001.
[8] J. Huhmann-Vincent, B.L. Scott, G.J. Kubas, Inorg. Chim. Acta 294 (1999) 240.
[9] T. Iwasa, H. Shimada, A. Takami, H. Matsuzaka, Y. Ishii, M. Hidai, Inorg. Chem. 38 (1999) 2851.
[10] A.J. Chalk, J. Halpern, J. Am. Chem. Soc. 81 (1959) 5846.
[11] G.B. Richter-Addo, P. Legzdins, Metal Nytrosyls, Oxford University Press, New York, 1992.
[12] H. Berke, P. Burger, Comments Inorg. Chem. 16 (1994) 279.
[13] B. Machura, Coord. Chem. Rev. 249 (2005) 2277.
[14] F.C. Giovanni, F. Gernot, Organometallics 26 (2007) 5815.
[15] B. George, A. Richter, L. Peter, Chem. Rev. 88 (1888) 991.
[16] A. Llamazares, H.W. Schmalle, H. Berke, Organometallics 20 (2001) 5277.
[17] D.V. Yaundolov, W.E. Steib, K.G. Caulton, Inorg. Chim. Acta 280 (1998) 125.
[18] D. Gusev, A. Llamazares, G. Artus, H. Jacobsen, H. Berke, Organometallics 18 (1999) 75.
[19] A. Choualeb, A.J. Lough, D.G. Gusev, Organometallics 26 (2007) 3509.
[20] P. Legzdins, S.F. Sayers, Chem. Eur. J. 3 (1997) 1579.
[21] P. Kundel, H. Berke, J. Organomet. Chem. 335 (1987) 353.
[22] N.V. Belkova, E.S. Shubina, A.V. Ionidis, L.M. Epstein, H. Jacobsen, A. Messmer, H. Berke, Inorg. Chem. 36 (1997) 1522.
[23] A. Messmer, H. Jacobsen, H. Berke, Chem. Eur. J. 5 (1999) 3341.
[24] D. Stefan, F. Gernot, Organometallics 15 (1996) 4547.
[25] F.W. Fee, M.C.W. Chan, K.K. Cheung, C.M.J. Che, Organomet. Chem. 563 (1998) 191.
[26] E. Bannwart, H. Jacobsen, F. Furno, H. Berke, Organometallics 19 (2000) 3605.
[27] L. Zhang, M.P. Gamasa, J. Gimeno, R.J. Carbajo, F. Lopez Ortis, M. Lanfranchi, A. Tiripicchio, Organometallics 15 (1996) 4274.
[28] S. Ye, W. Zhou, A. Masaaki, N. Takuma, C. Longfei, U. Kohei, O. Masatoshi, S. Yoichi, J. Am. Chem. Soc. 126 (2004) 7434.
[29] W.J. Huang, H. Berke, Chimia 59 (2005) 113.
[30] X.Y. Liu, K. Venkatesan, H.W. Schmalle, H. Berke, Organometallics 23 (2004) 3153.
[31] A. Choualeb, E. Maccaroni, O. Blacque, H.W. Schmalle, H. Berke, Organometallics 27 (2008) 3474.
[32] C. Lee, W. Yang, G. Parr, Phys. Rev. B 37 (1988) 785.
[33] B. Miehlich, A. Savin, H. Stoll, H. Preuss, Chem. Phys. Lett. 157 (1989) 200.
[34] A.D. Becke, J. Phys. Chem. 98 (1993) 5648.
[35] K. Fukui, J. Phys. Chem. 74 (1970) 4161.
[36] K. Fukui, Acc. Chem. Res. 14 (1981) 363.
[37] P.J. Hay, W.R. Wadt, J. Chem. Phys. 82 (1985) 299.
[38] J. Andzelm, S. Huzinaga, Gaussian Basis Sets for Molecular Calculations, Elsevier Science, New York, 1984.
[39] M.J. Frisch et al., GAUSSIAN 98, Revision A.9, Gaussian Inc., Pittsburgh, PA, 1998.
[40] S.W. Bi, Z.Y. Lin, R.F. Jordan, Organometallics 23 (2004) 4882.
[41] S.W. Bi, A. Ariafard, G. Jia, Z.Y. Lin, Organometallics 24 (2005) 680.
[42] A. Ariafard, S.W. Bi, Z.Y. Lin, Organometallics 24 (2005) 2241.
[43] A. Ariafard, Z.Y. Lin, Organometallics 24 (2005) 3800.
[44] S.W. Bi, S.F. Zhu, Z. Zhang, Z. Yuan, J. Organomet. Chem. 692 (2007) 3454.
[45] S.W. Bi, S.F. Zhu, Z. Zhang, Eur. J. Inorg. Chem. 14 (2007) 2046.

[46] S.W. Bi, Z. Zhang, S.F. Zhu, Chem. Phys. Lett. 431 (2006) 385.
[47] S.W. Bi, Q.M. Xie, X.R. Zhao, Y.Y. Zhao, X.J. Kong, J. Organomet. Chem. 693 (2008) 633.
[48] J.M. Gonzales, D.G. Musaev, K. Morokuma, Organometallics 24 (2005) 4908.
[49] V.P. Ananikov, N.V. Orlov, M.A. Kabeshov, I.P. Beletskaya, Z.A. Starikova, Organometallics 27 (2008) 4056.
[50] A.A.C. Braga, G. Ujaque, F. Maseras, Organometallics 25 (2006) 3647.
[51] T. Tuttle, D.Q. Wang, W. Thiel, Organometallics 25 (2006) 4504.